https://doi.org/10.33263/Materials21.064072

ISSN: 2668-5728 https://materials.international

Materials International

Article

Volume 2, Issue 2, Pages 0064-0072
2020

Received: 20.01.2020
Accepted: 06.03.2020
Published: 15.03.2020

Influence of pH on the photocatalytic activity of ZnO nanorods

M.J. Kadhim [1], M.A. Mahdi [1,*], J.J. Hassan [1]

[1] Department of Physics, College of Science, University of Basrah, Basrah, Iraq
* Correspondence: m.a.mahdi@uobasrah.edu.iq; Scopus ID: 37077680600

Abstract: Zinc oxide (ZnO) nanorods were prepeared on glass substrates through the chemical bath deposition (CBD) method. The growth of vertically array ZnO nanorods was promoted by seeding the substrates with ZnO nanoparticle layers. Surface morphology that investagated through field-emission scanning electron microscopy (FESEM) show that hexagonal ZnO nanorods (wurtzite) are formed with diameters ranging from 10 nm to 130 nm. The optical absorption of the grown ZnO nanorods exhibited high absorption edge with an energy gap of 3.26 eV. The photocatalytic activity of the prepared ZnO nanorods was investigated against methylene blue dye at room temperature using different pH values and UV exposure times. Degradation ratio of dye increased when irradiation time and pH were increased. The degradation ratio for dye with pH 6 increased from 42% to 89% when exposure time increased from 30 min to 240 min, whereas the degradation ratio of the dye with pH 11 increased from 65% to 94% under the same exposure time.

Keywords: zinc oxide, nanorods, photocatalyst.

1. Introduction

Photocatalysis for water treatments is a new technology used in purifying water. Many methods have been introduced for the removal of organic toxicity in water, including extraction, polymerization, electro-Fenton process, and photocatalytic degradation. Photocatalysis with one-dimensional nanomaterials with UV/visible light exposure has attracted interest in recently due to its high oxidation efficiency and excellent stability. One-dimensional semiconductors, such as nanowires, nanotubes, and nanorods, have received attention in recent years because of their unique properties, including high crystallinity, high surface-to-volume ratio, quantum confinement, and slow electron–hole recombination, which greatly enhance behavior when fabricating various electronic and optoelectronic devices [1, 2]. Recently, heterogeneous photocatalysis based on advanced oxidative processes has gained wide attention owing to its potential applications in environmental treatment [3]. Many researchers are focused on effectively removing or treating organic pollutants, which are the main pollutants contributing to environmental degradation. Photocatalysis can be defined as an acceleration of a photo-induced reaction with catalysts [4]. Photocatalysis is an effective process for reducing the oscillation rates of toxic organic compounds

Cite This Article: Kadhim, M.J.; Mahdi, M.A.; Hassan, J.J. Influence of pH on the photocatalytic activity of ZnO nanorods. Mat Int **2020**, 2, 0064-0072. https://doi.org/10.33263/Materials21.064072

and hazardous inorganic substances [5]. Photocatalysts undergo optical excitation by ultraviolet, visible, or near-infrared light depending on their energy band gaps and disrupt a wide range of waterborne microbes through a simple optical oxidation mechanism. Photocatalysts have many environmental applications; for example, they are often used as antimicrobial materials against many types of bacteria, viruses, and fungi [6] and for waste water treatment. Metal oxide semiconductors are considered good photocatalysts and can produce electron–hole pairs when exposed to UV or visible light [7, 8]. Metal oxides exhibit optical and electronic properties without change in structure. This feature is of major importance in heterogeneous photocatalysis owing to its electronic factors. Heterogenous photocatalysis depends on the molecular spectral analysis of absorbed molecules, so we focused on understanding the changes in the molecular structure caused by the absorption of molecules on solid wall surfaces [9]. The efficiency of photocatalysts can be enhanced by reducing the rapid recombination of charge carriers in metal oxides [10], and the important factors affecting the result of photocatalysis are catalytic dosage, pH, and dye concentration [11]. Many types of metal oxides, such as ZnO [12], TiO_2 [13], ZrO_2 [14], SnO_2 [15], α-Fe_2O_3 [16], and GeO [17], are used as photocatalysts and in degrading environmental pollutants. ZnO is an important metal oxide semiconductor because of its unique physical and chemical properties, such as wide band gap (3.37 eV) and high excitation energy (60 meV) [18] at room temperature. In addition, ZnO has high chemical stability and is environmentally friendly, low cost, and easy to synthesize in nanostructure forms [18, 19]. Furthermore, ZnO nanorods have high surface-to-volume ratios [20], thereby providing large surface areas for the absorption of UV and visible photons, which are important in the photocatalytic process [21]. In the current work, ZnO nanorods were prepared by the chemical bath deposition (CBD) method. The photocatalytic activities of the prepared ZnO nanorods were investigated under various pH values and UV exposure times.

2. Materials and Methods

2.1 Synthesis of ZnO nanorods

The ZnO seed layer is used to grow vertically aligned ZnO nanorods onto glass microscopy slide substrates. ZnO seed layer solution is prepared using a 5 mM zinc acetate dihydrate [$Zn(CH_3CO_2)_2{\cdot}2H_2O$] dissolved in 50 ml of ethanol and stirred for 3 h at room temperature. Glass substrates are cleaned with an ultra-sonicater type (Tefic Biotech Co., Limited) in hydrochloric acid, ethanol, and distilled water (DW) for 10 min each. Then, the prepared seed solution is casted on the cleaned glass substrates and dried at 50 °C. The seeded substrates are annealed at 350 °C for 1 h to grow ZnO nanoparticles and left to cool naturally to room temperature. ZnO nanorods are grown onto seeded glass substrates by the CBD method using 0.1 M of each zinc nitrate hexahydrate $Zn(NO_3)_2{\cdot}6H_2O$ and hexamine $C_6H_{12}N_4$ that dissolved individually in 25 ml of DW at 70 °C. Finally, the solutions are mixed, and seeded substrates are immersed vertically inside a beaker at 90 °C for 2 h. After ZnO nanorod preparation, the substrates are removed from the solution and rinsed inside DW and ethanol for several times, dried, and heat treated at 350 °C for 1 h.

2.2 Photocatalytic activity

The photocatalytic activity of prepared ZnO nanorods is investigated using methylene blue (MB) dye with concentration of 9 ppm. ZnO nanorod thin films are placed horizontally in the beaker containing 40 ml of MB dye and exposed to UV light (265 nm).

The photocatalytic activity of the ZnO nanorods is determined at various pH values and times of exposure. The degradation rate of MB dye is estimated using the following formula [22]:

$$degradation\ rate\% = \frac{A_o - A}{A_o} \times 100\% \quad (1)$$

where A_o is the absorbance at zero exposure time (t_o), and A is the absorbance at $\boldsymbol{t}$ time of exposure. The pH value of MB dye is controlled using NaOH and some drops of HNO_3 acid. The pH determines the surface charge of the photocatalytic activity, which makes the photocatalytic activity positive in the acidic medium and negative charge in the basal medium [23].

Degradation kinetics (k) of the MB dye can be described using the first-order Langmuir equation that is represented by [24]:

$$C = C_o e^{-kt} \quad (2)$$

where t is the time of the reaction, C_o is the initial concentration of MB dye, C is the concentration after exposure, and k is the first-order constant of the degradation reaction. The concentration is calculated according to Beer–Lambert's law [25].

$$A = \varepsilon\, C\, l \quad (3)$$

where A is the absorbance expressed, ε is the molar absorptivity, and l is the UV light path length (1 cm).

3. Results and Discussion

3.1 Surface morphology

Figure 1 shows the FESEM image of ZnO nanorods grown onto seeded glass substrates through the CBD method.

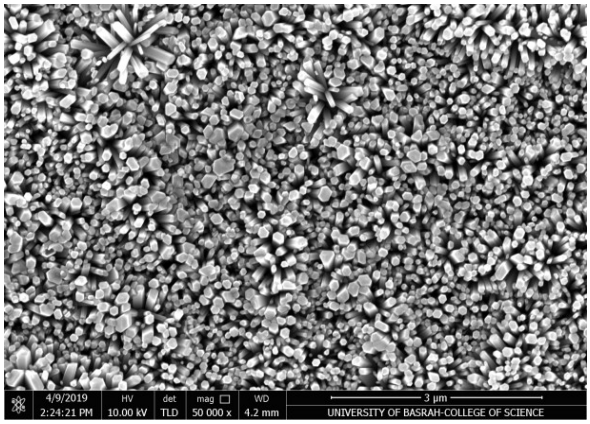

Figure 1. FESEM image of the grown ZnO nanorods thin film

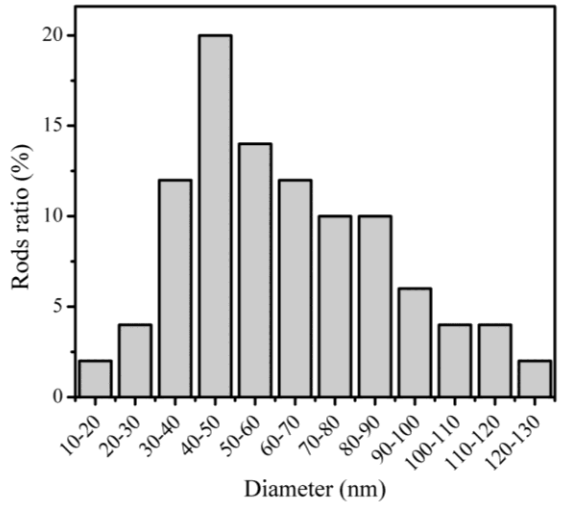

Figure 2. Statistical distribution of the grown ZnO nanorods thin film

The ZnO nanorods have perfect hexagonal shape and are aligned vertically on the substrates. The ZnO nanoparticle seed layer is of great importance in the vertical growth of ZnO nanorod arrays [26]. Figure 2 shows the statistical distribution of the ZnO nanorod with diameters with diameters of 10–130 nm. Notably, a large percentage of nanorods are distributed between 41 and 50 nm.

3.1 Optical properties

The optical absorption spectrum of ZnO nanorod thin film is displayed in Figure 3a. A strong absorption edge is present at a wavelength of 368 nm. The energy gap of the semiconductors can be estimated using the relationship between absorbance and incident photon energy ($h\upsilon$) for direct electron transition [27]:

$$ahv = A(h\upsilon - E_g)^{\frac{1}{2}} \quad (4)$$

where A is the constant and E_g is the energy gap. The estimated energy gap of ZnO nanorod thin films is 3.26 eV, which is close to the value obtained by I. Polat et al. (Fig. 3b) [28].

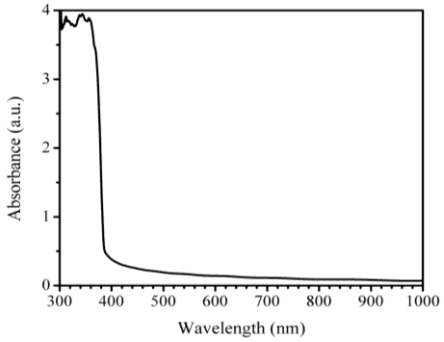

Figure 3a. UV-Vis absorption spectrum of the grown ZnO nanorods thin film

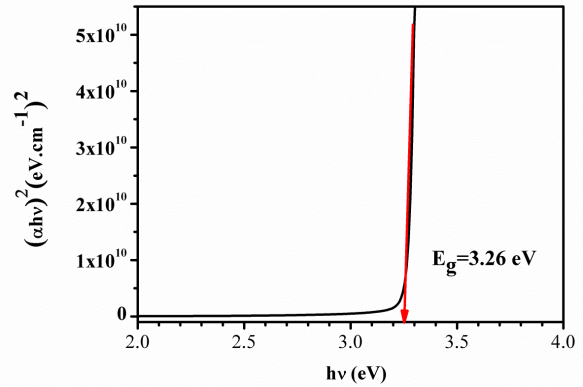

Figure 3b. $(\alpha.h\upsilon)^2$ vis. hυ of the grown ZnO nanorods thin film

3.3 Catalyst degradation

Dye is degraded by illuminating the catalyst with a photon possessing an energy higher than the energy gap. The photon excites the electrons from the valance band (VB) to the conduction band (CB) leaving holes. High oxidation potential of electrons in CB allows direct oxidation of dye in the reaction medium followed by the degradation process. Dye decay is caused by its interaction with free radicals (hydroxyl [$OH^{\cdot}$] and superoxide [$O_2^{\cdot}$]) produced by the catalyst. The interaction is shown as the following equations [7, 8]:

$$ZnO + h\upsilon \rightarrow ZnO\ (e_{CB}^{-} + h_{VB}^{+}) \quad (5)$$

$$ZnO(h^{+}) + H_2O \rightarrow ZnO + H^{+} + OH^{\cdot} \quad (6)$$

$$ZnO(h^{+}) + OH^{-} \rightarrow ZnO + OH^{\cdot} \quad (7)$$

$$ZnO(e^{-}) + O_2 \rightarrow ZnO + O_2^{\cdot -} \quad (8)$$

$$O_2^{\cdot -} \xrightarrow{H^{+}} HO_2^{\cdot} \quad (9)$$

$$Dye + h^{+} \rightarrow oxidation\ products \quad (10)$$

$$Dye + e^{-} \rightarrow reducation\ products \quad (11)$$

$$Dye + OH^{\cdot} \rightarrow degradation\ prodact \quad (12)$$

The effect of pH on the rate of degradation is studied for MB dye where pH value is of great importance to the efficiency of the photocatalytic degradation process. Figure 4(a–e) shows the absorbance of MB dye measured in different pH values (6–11) with various exposure times (30–240 min). As the absorbance of MB dye decreases, irradiation time increases. This result indicates increase in the degradation efficiency of photocatalysts [29]. Figure 5 showas the calibration plot of MB dye at a wavelength of 664 nm. Degradation rate (%) and k value with irradiation time for each pH are showed in Fig. 6 and obtaied values are listed in Table1. The molar absorptivity (ε) of MB dye is calculated through a calibration curve using different concentration, as shown in Figure 5. Figure 6a shows C/C_o plot versus the irradiation time of ZnO nanorod thin films for MB dyes with different pH values. However, the concentration of the MB dye decreases at increasing pH value and irradiation time in the pH range of 8–11 and shows an inversion behavior at a pH value of 6.

Figure 7 shows the relationship between the degradation rate of MB dye and irradiation time. Notably, degradation efficiency increases with irradiation time in the MB dyes regardless of their pH values. The degradation rate of the MB dye increases from 42% to 89% when pH is 6 and when irradiation time is increased from 30 min to 240 min. The degradation rates of MB dye under 240 min of UV irradiation are 71%, 77%, 87%, and 94% for pH values of 8, 9, 10, and 11, respectively. This behavior could be due to the increase in $OH^{\cdot}$ concentration, which acts with photo-generated holes as strong oxidants that lead to the degradation of MB dye [30]. The oxygen vacancy defects of catalytic materials induce new donor levels below its CB, which also work to improve photocatalytic activity and increase surface oxygen vacancy. Therefore, the surface recombination centers are decreased that in turn afford oxygen vacancies enough time to act as electron acceptors during the photocatalytic reaction and to reduce the recombination rate. Furthermore, oxygen vacancies can enable the adsorbed O_2 to capture photo-induced electrons and generate superoxide radical anions that

Many other researchers have worked on the similar process as listed in Table 2. However, a fundamental understanding of the effect of the degradation process, such as pH or morphology, is limited. Therefore, in the present study, the effects of pH and the photocatalytic responses of the prepared ZnO are evaluated by dye degradation. M. Sabbaghan et al. investigated the effect of template on morphology and photocatalytic properties of ZnO nanostructures. Their results

showed that the ZnO, nanocauliflower, nanorod-like, and nanosheet-like nanoparticles have 58%, 45%, 35%, 78%, and 55% morphology, respectively [27].

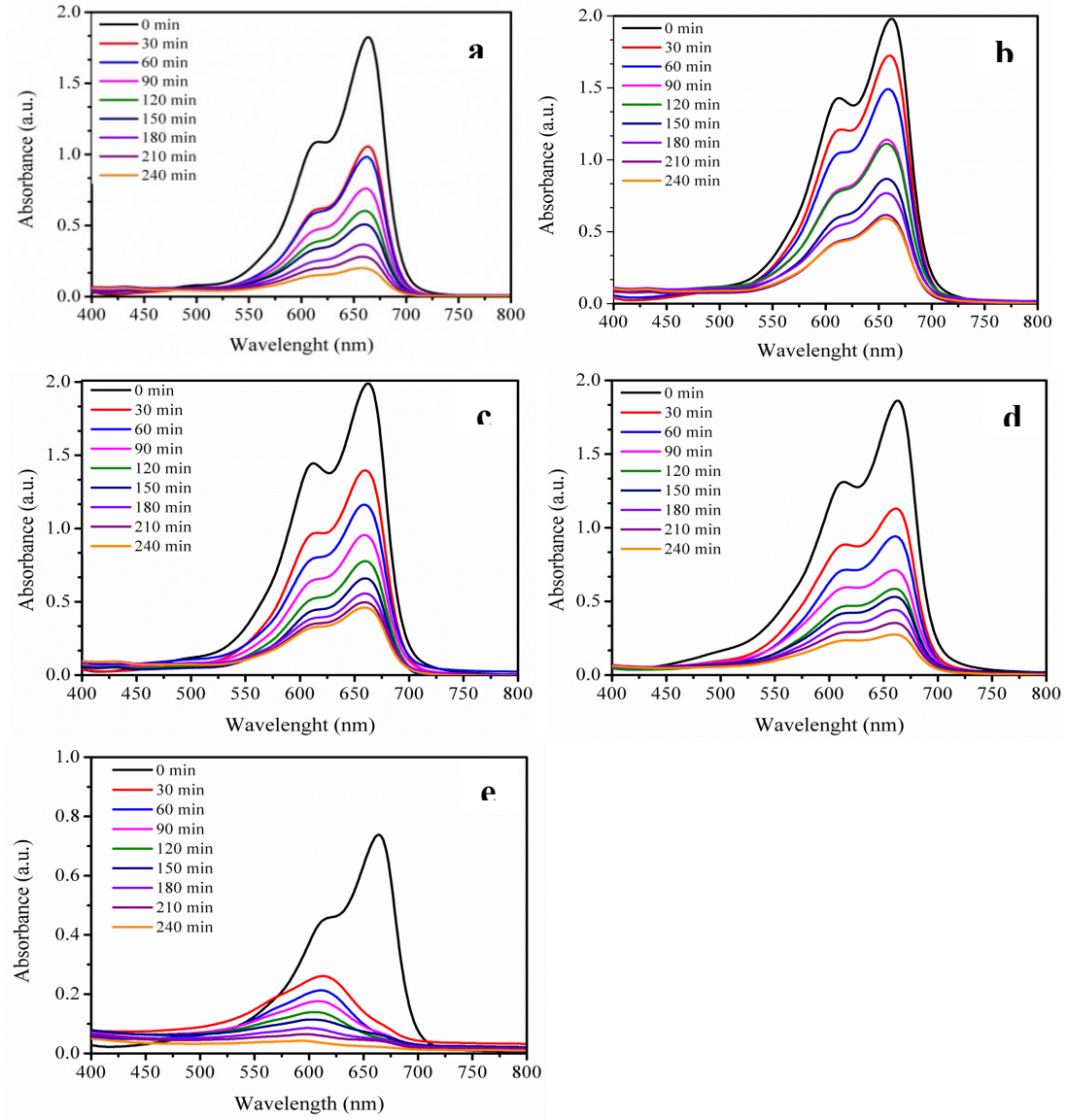

Figure 4. UV-VIS spectra of MB dye photocatalytic by ZnO nanorods thin film at (a) pH 6, (b) pH 8, (c) pH 9, (d) pH 10, and (e) pH 11

Table 1. Obtained values of degradation rate (%) and k with irradiation timeand pH.

pH	Degradation rate%								K min^{-1}
	30min	60min	90min	120min	150min	180min	210min	240min	
6	42	46	59	67	73	80	85	89	0.0086
8	13	25	43	45	57	62	70	71	0.0054
9	30	42	52	61	67	72	75	77	0.0060
10	40	50	63	70	73	77	82	87	0.0075
11	65	71	76	81	85	88	91	94	0.0099

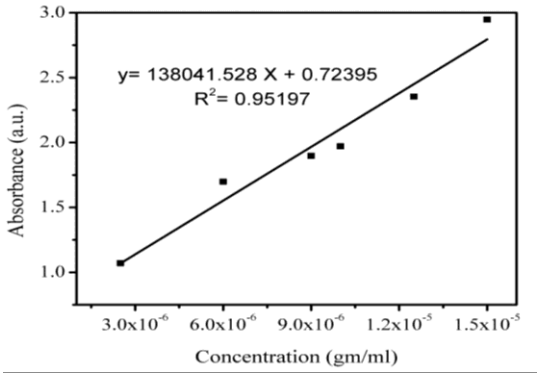

Fig.5: Calibration plot of MB dye at a wavelength of 664 nm

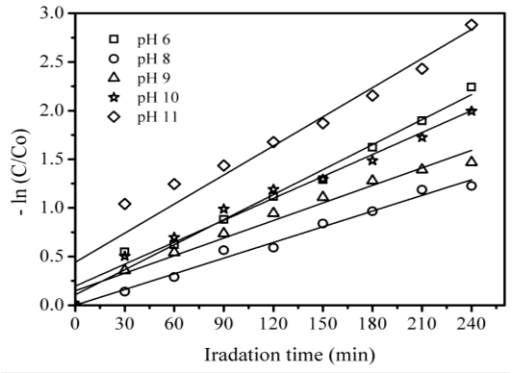

Fig.7: Variation of $-\ln (C/C_o)$ with irradiation time for different pH value

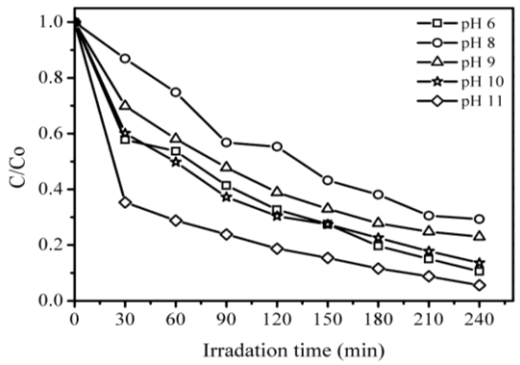

Fig.6: Kinetics of photocatalytic degradation by different pH value with irradiation time.

4. Conclusions

In the current study, ZnO nanorods were grown onto glass substrates through the CBD method. The ZnO nanorods were hexagonal in shape and in a vertical array on the substrates. The photocatalytic activity against MB dye was investigated under different pH values and UV-light irradiation times. The results show that the degradation rate of MB increased when pH value and irradiation time increased. the possible reasons for the enhancement of the photocatalytic activities of the grown ZnO nanorods were the increase in $OH^{\cdot}$ concentration after the increase in pH and ZnO nanorod surface defects due to oxygen vacancy. These defects induce donor energy levels below its CB which works in improving the photocatalytic activity. MB dye on the surface of the ZnO nanorods degraded because of the hydroxyl radical and photo-generated holes, which are strong oxidants. Furthermore, surface oxygen vacancy decreases the surface recombination centers that afford oxygen vacancies enough time to act as electron acceptors during the photocatalytic reaction and to reduce the recombination rate.

Table 2. Comparison obtained results of degradation rate (%) by other published works

Photocatalysts	morphology	Degradation rate (%)	Time of irradiation (min)	pH	Reference
ZnO	nanorods	89	240	6	Current work
		71		8	
		77		9	
		87		10	
		94		11	
		6.58	90	--	32
	nanoparticles	49	60	9	33
	nanocrystal	91	240	--	34
	nanoparticles	65			
	nanoparticles	58	80	--	29
		45			
	nanocauliflower	35			
	nanorod-like	78			
	nanosheet-like	55			
	flower-like	97	20	13	35
	nanopowder	7.169	120	4.5	36
		47.63		10.5	
	nanoparticles	60	240	4	37
		42		8	
		81		11	
Ce/ZnO	nanorods	7.56	90	--	32
ZnO/Go	nanoparticles	98.5	15	9	33

Funding

This research received no external funding

Acknowledgments

The authors declare no conflict of interest.

Conflicts of Interest

The authors declare no acknowledgments.

References

1. Abdul-Hameed, A.A; Mahdi, M.A.; Ali, B Selman, A. M; Al-Taay, H.F; Jennings, P. Lee, W.J. Fabrication of a high sensitivity and fast response self-powered photosensor based on a core-shell silicon nanowire homojunction. *Superlattices Microstruct*, **2018**, *Volume 116*, pp. 27-35. https://doi.org/10.1016/j.spmi.2018.02.003

2. Al-Taay, H.F; Mahdi, M.A; Parlevliet , D.; Jennings, P. Controlling the diameter of silicon nanowires grown using a tin catalyst. *Mat. Sci. Semicon. Proc.*, **2013**, *Volume 16, Issue 1*, pp.15-22. https://doi.org/10.1016/j.mssp.2012.07.006

3. You, J.; Guo,Y.; Guo, R.; Liu, X. A review of visible light-active photocatalysts for water disinfection: Features and prospects. *Chem.Eng. J.*, **2019**, *Volume 373*, pp.624–641. https://doi.org/10.1016/j.cej.2019.05.071

4. Gerven, T.V.; Mul, G.; Moulijn, J.; Stankiewicz, A. A review of intensification of photocatalytic processes. *Chem.Eng. Proc.*, **2007**, *Volume 46, Issue 4*, pp. 781–789. https://doi.org/10.1016/j.cep.2007.05.012

5. Baruah, S.; Rafique, R.F.; Dutta, J. Visible light photocatalysisby tailoring crystal defects inzinc oxide nanostructures. *Nano*, **2008**, *Volume 3, Issue 5*, pp. 399-407. https://doi.org/10.1142/S179329200800126X

6. Liou, J.W.; Chang, H.H. Bactericidal effects and mechanisms of visible light-responsive titanium dioxide photocatalysts on pathogenic bacteria. *Arch. Immunol.*

Ther. Exp., **2012**, *Volume 60*, pp. 267–275. https://doi.org/10.1007/s00005-012-0178-x

7. Saravanan, R.; Gupta, V.J.; Narayanan, V.; Stephen, A. Comparative study on photocatalytic activity of ZnO prepared by different methods. *J.Mol. Liq.*, **2013**, *Volume 181*, pp. 133-141. https://doi.org/10.1016/j.molliq.2013.02.023

8. Konstantinou, I.K.; Albanis, T.A.; TiO_2 -assisted photocatalytic degradation of azo dyes inaqueous solution: kinetic and mechanistic investigations: A review. *Appl.Catal. B: Environ.*, **2004**, *Volume 49, Issue 1*, pp. 1-14. https://doi.org/10.1016/j.apcatb.2003.11.010

9. Suib, S.L. New And Future Development in Catalysis/Solar Photocatalysis, Chapter 1, pp.2-3 University of Connecticut. Storrs, CT 06269, 2013.

10. Zhang, F.; Chen, J.; Zhang, X.; Gao, W.; Jin, R.; Guan, N.; Li, Y. Synthesis of Titania-Supported Platinum Catalyst: The Effect of pH on Morphology Control and Valence State during Photodeposition. *Langmuir*, **2004**, *Volume 20 , Issue 21*, pp. 9329-9334. https://doi.org/10.1021/la049394o

11. Devadi, M.A.; Krishna, M.; Murthy, H.N.; Sathyanarayana, B.S. Statistical Optimization for Photocatalytic Degradation of Methylene Blue by Ag-TiO2 Nanoparticles. *Procedia Mater Sci*, **2014**, *Volume 5*, pp. 612-621. https://doi.org/10.1016/j.mspro.2014.07.307

12. Leea, K.M.; Lai, C.W.; Ngai, K.S.; Juan, J.C. Recent developments of zinc oxide based photocatalyst in watertreatment technology: A review. *Water Res.*, **2016**, *Volume 88*, pp. 428-448. https://doi.org/10.1016/j.watres.2015.09.045

13. Bellardita, M.; Paola, A.D.; Megna, B.; Palmisano, L. Determination of the crystallinity of TiO2 photocatalysts. *J.Photochem. Photobiol. A: Chem.*, **2018**, *Volume 367*, pp. 312-320. https://doi.org/10.1016/j.jphotochem.2018.08.042

14. García-López, E.; Marcì, G.; Pomilla, F.R.; Paganini, M.C.; Gionco, C.; Giamello, E.; Palmisano, L. ZrO2 Based materials as photocatalysts for 2-propanol oxidation by using UV and solar light irradiation and tests for CO2 reduction. *Catal.Today*, **2018**, *Volume 313*, pp. 100-105. https://doi.org/10.1016/j.cattod.2018.01.030

15. Zhao, D.; Wu, X. Nanoparticles assembled SnO2 nanosheet photocatalysts for wastewater purification, *Mat. Lett.*, **2018**, *Volume 210*, pp. 354-357. https://doi.org/10.1016/j.matlet.2017.09.068

16. Mishra, M.; Chun, D. -M. α-Fe2O3 As a Photocatalytic material: A Review. *Appl. Catal. A*, **2015**, *Volume 498*, pp. 126-145. https://doi.org/10.1016/j.apcata.2015.03.023

17. Lin, Z.; Du, C.; Yan, B.; Yang, G. Two-dimensional amorphous CoO photocatalyst for efficient overall water splitting with high stability. *J.Catal.*, **2019**, *Volume 372*, pp. 299-310. https://doi.org/10.1016/j.jcat.2019.03.025

18. Hassan, J.J.; Mahdi, M.A.; Asmiet Ramizy, A.; Abu Hassan, H.; Hassan, Z. Fabrication and characterization of ZnO nanorods/p-6H–SiC heterojunction LED by microwave-assisted chemical bath deposition. *Superlattices Microstruc.*, **2013**, *Volume 53*, pp. 31-38. https://doi.org/10.1016/j.spmi.2012.09.013

19. Akhavan, O.; Mehrabian, M.; Mirabbaszadeh, K.; Azimirad, R. Hydrothermal synthesis of ZnO nanorods arrays for photocatalytic inactivation of bacteria. *J.Phys. D: Appl.Phys.*, **2009**, *Volume 42, Issue 32*, pp. 225305. https://doi.org/10.1088/0022-727/42/22/225305

20. Hassan, J.J.; Mahdi, M.A.; Chin, C.W.; Abu-Hassan, H.; Hassan, Z. A high-sensitivity room-temperature hydrogen gas sensor based on oblique and vertical ZnO nanorod arrays. *Sensor. Actuat.B*, **2013**, *Volume 176*, pp. 360– 367. https://doi.org/10.1016/j.snb.2012.09.081

21.Talebian, N.; Amininezhad, S.M.; Doudi, M. Controllable synthesis of ZnO nanoparticles and their morphology-dependent antibacterial and optical properties. *J. Photochem. Photobio. B: Biol.*, **2013**, *Volume 120*, pp. 66-73. https://doi.org/10.1016/j.jphotobiol.2013.01.004

22. Raghu, S.; Lee, C.W.; Chellammal, S.; Palanichamy, S.; Bash, C.A. Evaluation of electrochemical oxidation techniques for degradation of dyeeffluents—A comparative approach. *J. Hazard. Mate.*, **2009**, *Volume 171, Issue 1-3*, pp. 748-754. https://doi.org/10.1016/j.jhazmat.2009.06.063

23. Kumar, A.; Pandey, G. A review on the factors affecting the photocatalytic degradation of hazardous materials. *Mat. Sci. & Eng. Int. J.*, **2017**, *Volume 1*, pp. 106-114. https://doi.org/10.15406/mseij.2017.01.00018

24. Houa, A.; Lachheb, H.; Ksibi, M.; Elaloui, E.; Guillard, C.; Herrman, J.-M. Photocatalytic degradation pathway of methylene blue in water, *Appl. Catal. B: Environ.,* **2001**, *Volume 31*, pp. 145-157. https://doi.org/10.1016/S0926-3373(00)00276-9

25. Gholivand, M.B.; Ghasemi, J.B.; Saaidpour, S.; Mohajeri, A. Spectrophotometric study of the effects of surfactants and ethanolon the acidity constants of fluorescein, *Spectrochim. Acta Part A*, **2008**, *Volume 71*, pp. 1158–1165. https://doi.org/10.1016/j.saa.2008.03.010

26. Hassan, J.J.; Mahdi, M.A.; Chin, C.W.; Hassan, Z.; Abu-Hassan, H. Microwave assisted chemical bath deposition of vertically aligned ZnO nanorods on avariety of substrates seeded by PVA–Zn(OH)2

nanocomposites. *Appl. Surf. Sci.*, **2012**, *Volume 258*, pp. 4467–4472. https://doi.org/10.1016/j.apsusc.2012.01.007

27. Jiang, H.; Endo, H.; Natori, H.; Nagai, M.; Kobayashi, K. Fabrication and efficient photocatalytic degradation of methylene blue over CuO/BiVO4composite under visible-light irradiation. *Mat. Res. Bull.*, **2009**, *Volume 44, Issue 3*, pp. 700-706. https://doi.org/10.1016/j.materresbull.2008.06.007

28. Polat, I.; Yılmaz, S.; Bacaksız, E.; Atasoy, Y.; Tomakin, M. Synthesis and fabrication of Mg-doped ZnO-based dye-sensitized solar cells. *J. Mat. Sci.Mat. Electro.*, **2014**, *Volume 25, Issue 10*, pp. 3173–3178. http://dx.doi.org/10.1007/s10854-014-2000-5

29. Sabbaghan, M.; Firooz, A.A.; Ahmadi, V.J. The effect of template on morphology, optical and photocatalytic properties of ZnO nanostructures. *J. Mol. Liq.*, **2012**, *Volume 175*, pp. 135-140. https://doi.org/10.1016/j.molliq.2012.08.019

30. Saravanan, R.; Thirumal, E.; Gupta, V.K.; Narayanan, V.; Stephen, A. The photocatalytic activity of ZnO prepared by simple thermal decompositionmethod at various temperatures. *J. Mol. Liq.*, **2013**, *Volume 177*, pp. 394-401. https://doi.org/10.1016/j.molliq.2012.10.018

31. Wang, C.; Wu, D.; Wang, P.; Ao, Y.; Hou, J.; Qian, J. Effect of oxygen vacancy on enhanced photocatalyticactivity of reduced ZnO nanorod arrays. *Appl. Surf. Sci.*, **2015**, *Volume 325*, pp. 112-116. https://doi.org/10.1016/j.apsusc.2014.11.003

32. Faisal, M.; Ismail, A.A.; Ibrahim, A.A.; Bouzid, H.; Al-Sayari, S.A. Highly efficient photocatalyst based on Ce doped ZnO nanorods:Controllable synthesis and enhanced photocatalytic activity. *Chem. Eng. J.*, **2013**, *Volume 229*, pp. 225-233. https://doi.org/10.1016/j.cej.2013.06.004

33. Raizad, P.; Sudhaik, A.; Singh, P. Photocatalytic water decontamination using graphene and ZnO coupled photocatalysts: A review. *Mat. Sci. Energy Technol.*, **2019**, *Volume 2*, pp. 509-525. https://doi.org/10.1016/j.mset.2019.04.007

34. Wang, Y.; Yang, J.; Li, Y.; Jiang, T.; Chen, J.; Wang, J. Controllable preparation of ZnO nanostructure using hydrothermal-electrodeposited method and its properties. *Mat. Chem. Phys.*, **2015**, *Volume 153*, pp. 266-273. https://doi.org/10.1016/j.matchemphys.2015.01.013

35. Wang, Y.; Yang, Y.; Xi, L.; Zhang, X.; Jia, M.; Xu, H.; Wu, H. A simple hydrothermal synthesis of flower-like ZnO microspheres and their improved photocatalytic activity. *Mat. Lett.*, **2016**, *Volume 180*, pp. 55–58. https://doi.org/10.1016/j.matlet.2016.05.107

36. Singh, R.; Dutta, S. The role of pH and nitrate concentration in the wet chemical growth of nano-rods shaped ZnO photocatalyst. *Nano-Structures & Nano-Objects*, **2019**, *Volume 18*, pp. 100-250. https://doi.org/10.1016/j.nanoso.2019.01.009

37. Kazeminezhad, I.; Sadollahkhani, A. Influence of pH on the photocatalytic activity of ZnO nanoparticles. *J. Mat. Sci.: Mat. Electro.*, **2016**, *Volume 27, Issue 5*, pp. 4206-4215. https://doi.org/10.1007/s10854-016-4284-0